Journal of Sound and Vibration (2002) **249**(5), 885–897
doi:10.1006/jsvi.2001.3875, available online at http://www.idealibrary.com on IDEAL®

ACOUSTIC POWER SUPPRESSION OF A PANEL STRUCTURE USING H_∞ OUTPUT FEEDBACK CONTROL

S. Sivrioglu

Mechanical Engineering Laboratory, Sound and Vibration Division, Namiki 1-2, *Tsukuba-shi* 305-8564, *Japan. E-mail*: *selim@mec2.tm.chiba-u.ac.jp*

N. Tanaka

Tokyo Metropolitan Institute of Technology, 6-6 *Asahigaoka*, *Hino-shi* 191-0065, *Tokyo*, *Japan*

and

I. Yuksek

Faculty of Mechanical Engineering, *Yildiz Technical University*, *Istanbul*, *Turkey*

(*Received* 21 *November* 2000, *and in final form* 30 *May* 2001)

This paper presents a robust control system design for suppressing the radiated acoustic power emitted from a vibrating planar structure, and spillover effect caused by neglected high-frequency modes. A state-space model of a simply supported panel structure is derived and an output equation is formed based on the one-dimensional PVDF film sensors. An output feedback H_∞ control is designed by introducing a multiplicative perturbation which represents unmodelled high-frequency dynamics in the control system. The simulation and experimental results demonstrated significant decrease in sound radiation for the considered structural power modes in control.

1. INTRODUCTION

Active control of sound radiation emitted from vibrating structures has been intensively investigated using distributed parameter sensors and piezoceramic actuators in recent years. One of the approaches used for the suppression of structure-borne noise is based on the vibration control, in which the vibration of an objective structure is controlled to suppress the noise radiated from it. With respect to this approach, the earlier works [1, 2] demonstrated the use of piezoactuators and piezoelectric Polyvinylidenedifluoride (PVDF) film sensors in active control of sound radiation. Adaptive control of a panel structure with attached PVDF sensors is studied using both feedforward and feedback control in references [3–5]. In a most recent research [6], the use of adaptive sensoriactuators is presented for structural acoustic control. Distributed parameter PVDF film sensors and piezoelectric actuators are used to create adaptive or smart structures [7]. Besides sensors and actuators, controllers also play a central role in active structural control. Robustness of a structural control system may sometimes be an issue due to the disturbance effect of high order structural modes even if the most advanced sensors and actuators are employed with the structure.

0022-460X/02/050885 + 13 $35.00/0

In this study, a systematic control design based on a state-space model of a panel structure is presented. Although a velocity feedback is mostly preferred due to its simplicity to add damping into a control system, there are some advantages to design a dynamic controller. First, a dynamic controller itself is a system in a state-space form and involves some systematic design steps with knowledge of the plant parameters. Therefore, in each step such as modelling, controller design, closed-loop simulations and experiments one can have the ability to design a desired robust controller which satisfies stability and performance requirements. Second, a direct displacement feedback to the controller is possible without any derivation of the sensor signal. Therefore, noise-related problems caused by the derivation of the sensor signal is avoided.

This paper begins with the derivation of an output equation based on distributed sensor outputs. For the completeness of the study, a state-space equation describing the motion of a distributed parameter structure is derived and transformed to suppress acoustic power. H_∞ controller design is explained extensively with the control objectives and the selection of frequency weighting filters. In addition, modelling issue for distributed parameter structures is discussed for a robust control design to avoid the effects of high order frequency modes. Finally, experiments on active modal control are conducted using H_∞ robust controllers, showing a significant reduction of the targeted modal amplitude without causing instability of the control system.

2. PANEL STRUCTURE

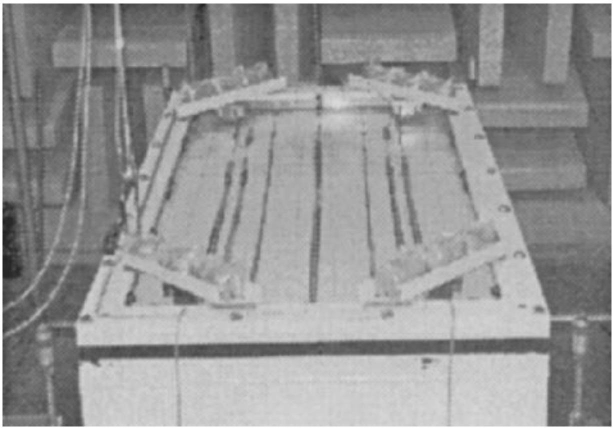

Figure 1. Picture of the experimental panel structure.

2.1. DERIVATION OF THE MODAL OUTPUT EQUATION

PVDF sensors can be shaped so as to act as spatial filters which only observe certain modes. References [8, 9] described the design procedure of PVDF sensors for a certain frequency range by separating the modes of a panel structure into modal groups. Basically, the total charge produced by the PVDF sensors is computed using modal displacements of the distributed parameter structure for each group of the modes. In reference [10], the PVDF sensor outputs were combined as an output equation of the state space in order to design an output feedback H_∞ control for the panel structure. Following reference [8], the sensor output amplitude is expressed as

$$\tilde{y} = q_{nj} \sum_{m_j=1}^{N_m} x_j(m_j, n_j)\, b_j(m_j, n_j)\, c_j(m_j), \tag{1}$$

where q_{n_j} is the weight factor, $x_j(m_j, n_j)$ is the amplitude of the modal displacement. m_j and n_j denote the modal indices in the x and y directions of the plate in the frequency range of interest. N_m shows the total number of vibration modes. In this design, the PVDF film sensors are placed in the y direction of the plate. Here, $b_j(m_j, n_j)$ and $c_j(m_j)$ are defined as

$$b_j(m_j, n_j) = L_y \Gamma_0 \left(e_{32} \left(\frac{m_j \pi}{L_x} \right)^2 + e_{31} \left(\frac{n_j \pi}{L_y} \right)^2 \right),$$

$$c_j(m_j) = \sin \frac{m_j \pi}{L_x} \gamma, \tag{2}$$

where j denotes the mode number, e_{31}, e_{32} are the piezoelectric stress/charge coefficients, and Γ_0 is the shaping constant of the film sensor. In practice, the value of the shaping constant depends on the gain of charge amplifier, the thickness, area and material of the PVDF film. L_x and L_y are the width and the length of the plate. γ denotes the position of the film sensor in the x-axis. For four different structural modes such as odd/odd, odd/even, even/odd, and even/even, four sets of distributed parameter sensors should be designed. The outputs of each set are arranged as

$$y_{oo} = \sum_{i=1}^{n_{oo}} \tilde{y}_i^{(oo)}, \quad y_{oe} = \sum_{i=1}^{n_{oe}} \tilde{y}_i^{(oe)}, \quad y_{eo} = \sum_{i=1}^{n_{eo}} \tilde{y}_i^{(eo)}, \quad y_{ee} = \sum_{i=1}^{n_{ee}} \tilde{y}_i^{(ee)}. \tag{3}$$

Here n_{oo}, n_{oe}, n_{eo}, and n_{ee} denote the necessary number of sensors in order to separate each group of modes up to a prescribed frequency. The output equation can be obtained using the modal displacements with corresponding weighting factors computed using sensor shape functions. The final form of the output equation for the state-space equation is obtained as

$$y = \begin{bmatrix} y_{oo}(1)\ 0\ y_{oo}(2)\ 0 & \cdots & y_{oo}(N_m)\ 0 \\ y_{oe}(1)\ 0\ y_{oe}(2)\ 0 & \cdots & y_{oe}(N_m)\ 0 \\ y_{eo}(1)\ 0\ y_{eo}(2)\ 0 & \cdots & y_{eo}(N_m)\ 0 \\ y_{ee}(1)\ 0\ y_{ee}(2)\ 0 & \cdots & y_{ee}(N_m)\ 0 \end{bmatrix} \begin{bmatrix} \bar{x}_1 \\ \dot{\bar{x}}_1 \\ \vdots \\ \bar{x}_{N_m} \\ \dot{\bar{x}}_{N_m} \end{bmatrix}, \tag{4}$$

where $\bar{x}_1 \cdots \bar{x}_{N_m}$ and $\dot{\bar{x}}_1 \cdots \dot{\bar{x}}_{N_m}$ are the modal amplitudes and the modal velocities respectively.

2.2. DERIVATION OF THE STATE-SPACE EQUATION

Consider the following equation for a one-dimensional distributed parameter flexible system:

$$M\ddot{w}(x, t) + 2\xi L^{1/2}\, \dot{w}(x, t) + Lw(x, t) = U(x, t), \tag{5}$$

where $w(x, t)$ is the displacement at location x on the structure at time t in response to the applied force U. Here, M and ξ represent the mass per unit area and the damping constant respectively. L is assumed to be a time-invariant positive differential operator. The eigenvalue problem is expressed as

$$L\psi_n = \lambda_n M\psi_n, \tag{6}$$

where λ_n is the nth eigenvalue, and ψ_n is the eigenfunction. The eigenvalues are related to the undamped natural frequencies ω_n as follows:

$$\lambda_n = \omega_n^2. \tag{7}$$

The displacement on the structure can be expressed as

$$w(x,t) = \sum_{i=1}^{\infty} x_i(t)\psi_i(x), \tag{8}$$

where $x_i(t)$ is the amplitude of ith mode and $\psi_i(x)$ is the value of the associated mode shape function. On substituting equation (8) into equation (5) with some computation, the equation of motion for the nth modes is obtained as

$$\ddot{x}_n(t) + 2\xi\omega_n\dot{x}_n(t) + \omega_n^2 x_n(t) = \int_s \psi_n(x)U(x,t). \tag{9}$$

From equation (9), the state-space equation for the nth mode has the form

$$\dot{\underline{x}}_n(t) = A_n\underline{x}_n(t) + B_n u(t) + D_n v(t), \tag{10}$$

where $\underline{x}_n$ is the state vector, u is the control input, and v is the disturbance input. The state vector and matrices are

$$\underline{x}_n(t) = \begin{bmatrix} x_n(t) \\ \dot{x}_n(t) \end{bmatrix}, \qquad A_n = \begin{bmatrix} 0 & 1 \\ -\omega_n^2 & -2\xi\omega_n \end{bmatrix},$$
$$B_n = \begin{bmatrix} 0 & 0 & \cdots & 0 \\ \tilde{\psi}_{n,1} & \tilde{\psi}_{n,2} & \cdots & \tilde{\psi}_{n,N_u} \end{bmatrix}, \qquad D_n = \begin{bmatrix} 0 & 0 & \cdots & 0 \\ \bar{\psi}_{n,1} & \bar{\psi}_{n,2} & \cdots & \bar{\psi}_{n,N_v} \end{bmatrix}, \tag{11}$$

where $\tilde{\psi}_{n,i}$, and $\bar{\psi}_{n,i}$ are the value of the mode shape function at the control force and disturbance force application point respectively. N_u and N_v represent the number of control and disturbance forces respectively. In general, the state-space equations for N_m structural modes can be written as

$$\dot{x}(t) = Ax(t) + Bu(t) + Dv(t), \tag{12}$$

where

$$x(t) = \begin{bmatrix} \underline{x}_1(t) \\ \underline{x}_2(t) \\ \vdots \\ \underline{x}_{N_m}(t) \end{bmatrix}, \qquad A = \begin{bmatrix} A_1 & & 0 \\ & A_2 & \\ & & \ddots & \\ 0 & & & A_{N_m} \end{bmatrix}, \qquad B = \begin{bmatrix} B_1 \\ B_2 \\ \vdots \\ B_{N_m} \end{bmatrix}, \qquad D = \begin{bmatrix} D_1 \\ D_2 \\ \vdots \\ D_{N_m} \end{bmatrix}. \tag{13}$$

2.3. ACOUSTIC POWER CONTROL

Equation (12) is not suitable for attenuating the acoustic power radiated from a vibrating structure. A transformation is necessary to minimize the acoustic power rather than to minimize vibration in a distributed parameter structure. With this aim, the acoustic power transform matrix is computed as

$$R_{ij} = \frac{\omega^3 \rho}{4\pi} \int_s \int_s \psi_i(r_2) \frac{\sin kr}{r} \psi_j(r_1)\, \mathrm{d}r_2\, \mathrm{d}r_1. \tag{14}$$

A factored form of R is given as

$$R = Q\Lambda Q^{-1}, \tag{15}$$

where Q is the orthogonal transform matrix, whose columns are the eigenvectors of R and Λ is the diagonal matrix of eignevalues. In order to minimize acoustic power, equation (12) is transformed to

$$\dot{\bar{x}}(t) = \bar{A}\bar{x}(t) + \bar{B}u(t) + \bar{D}v(t), \tag{16}$$

where

$$\bar{x}(t) = Q_e^{-1} x(t), \quad \bar{A} = Q_e^{-1} A Q_e, \quad \bar{B} = Q_e^{-1} B, \quad \bar{D} = Q_e^{-1} D. \tag{17}$$

Here, Q_e represents the $(2N_m \times 2N_m)$ expanded form of the orthogonal transform matrix given in equation (15).

3. H_∞ CONTROL DESIGN

3.1. PLANT AND UNCERTAINTY DEFINITION

H_∞ control theory is a well-established theory for feedback control [11] and some design tools [12] are available commercially in order to design an H_∞ controller. The theory will not be repeated here but the preparation for control design will be given extensively.

Theoretically, there are infinite number of modes in a distributed parameter system. On the other hand, a state-space equation which includes the plant dynamics up to the considered highest mode is necessary in order to design a controller. Although low-frequency modes dominate large amounts of modal contributions in a distributed parameter system, the frequency range selected for state space should be large enough to describe distributed parameter system dynamics so that the effect of higher modes which are not included in state space should be negligible.

Consider the panel structure as a control system depicted in Figure 2. The structural modes of this panel are presented in Table 1. It is assumed that 500 Hz is far enough for the state space to neglect effects of high order modes. Since modal filtering of the acoustic power

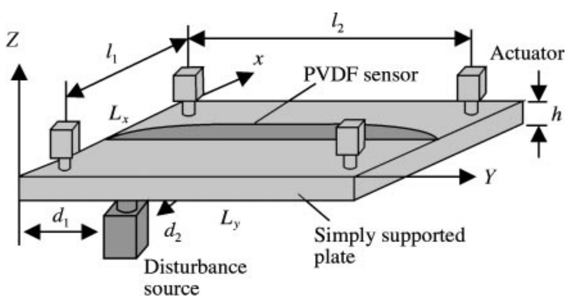

Figure 2. A simply supported panel structure.

TABLE 1

Vibration modes of the panel structure up to 500 Hz

Mode no.	Mode	Frequency	Mode no.	Mode	Frequency
1	(1,1)	35·292	12	(3,2)	283·588
2	(1,2)	55·716	13	(2,5)	284·136
3	(1,3)	89·756	14	(3,3)	317·628
4	(2,1)	120·744	15	(2,6)	359·024
5	(1,4)	137·412	16	(1,7)	362·077
6	(2,2)	141·168	17	(3,4)	365·284
7	(2,3)	175·208	18	(3,5)	426·556
8	(1,5)	198·684	19	(2,7)	447·529
9	(2,4)	222·864	20	(4,1)	462·551
10	(3,1)	263·164	21	(1,8)	464·198
11	(1,6)	273·573	22	(4,2)	482·975

modes is possible using PVDF sensors, each mode group such as odd/odd, odd/even, even/odd and even/even modes of the panel structure become independent of each other. Therefore, the state-space equations for each mode group may be formed in order to design four modal controllers. The state-space equation is obtained as

$$\dot{\bar{x}}_f^{(i)} = \bar{A}_f^{(i)} \bar{x}_f^{(i)} + \bar{B}_f^{(i)} u + \bar{D}_f^{(i)} v,$$

$$y_f^{(i)} = \bar{C}_f^{(i)} \bar{x}_f^{(i)} \quad (i = 1, \dots, 4), \tag{18}$$

where the dimensions of matrices are $\bar{A}_f^{(1)} \in \mathbb{R}^{14\times 14}$, $\bar{A}_f^{(2)} \in \mathbb{R}^{12\times 12}$, $\bar{A}_f^{(3)} \in \mathbb{R}^{10\times 10}$, $\bar{A}_f^{(4)} \in \mathbb{R}^{8\times 8}$, $\bar{B}_f^{(1)} \in \mathbb{R}^{14\times 4}$, $\bar{B}_f^{(2)} \in \mathbb{R}^{12\times 4}$, $\bar{B}_f^{(3)} \in \mathbb{R}^{10\times 4}$, $\bar{B}_f^{(4)} \in \mathbb{R}^{8\times 4}$, $\bar{C}_f^{(1)} \in \mathbb{R}^{4\times 14}$, $\bar{C}_f^{(2)} \in \mathbb{R}^{4\times 12}$, $\bar{C}_f^{(3)} \in \mathbb{R}^{4\times 10}$, $\bar{C}_f^{(4)} \in \mathbb{R}^{4\times 8}$, $\bar{D}_f^{(1)} \in \mathbb{R}^{14\times 1}$, $\bar{D}_f^{(2)} \in \mathbb{R}^{12\times 1}$, $\bar{D}_f^{(3)} \in \mathbb{R}^{10\times 1}$, $\bar{D}_f^{(4)} \in \mathbb{R}^{8\times 1}$. Note that the mode group numbers ($i = 1, \dots, 4$) correspond to the odd/odd, odd/even, even/odd and even/even modes respectively. Here, f indicates a full order modelling consideration of the plate up to 500 Hz frequency range. It is possible to design H_∞ controllers with high order using the full order state-space model but current DSP speeds are limited to implement high order controllers. A model reduction is inevitable for control design. For this reason, controllers will be designed for the frequency range of 150 Hz with six vibration modes. In this frequency range, there are two odd/odd, two odd/even, one even/odd and one even/even mode. The reduced order state-space equations of the plate for each mode group are formed as

$$\dot{\bar{x}}_r^{(i)} = \bar{A}_r^{(i)} \bar{x}_r^{(i)} + \bar{B}_r^{(i)} u + \bar{D}_r^{(i)} v,$$

$$y_r^{(i)} = \bar{C}_r^{(i)} \bar{x}_r^{(i)} \quad (i = 1, \dots, 4), \tag{19}$$

where $\bar{A}_r^{(1)}$, $\bar{A}_r^{(2)} \in \mathbb{R}^{4\times 4}$, $\bar{A}_r^{(3)}$, $\bar{A}_r^{(4)} \in \mathbb{R}^{2\times 2}$, $\bar{B}_r^{(1)}$, $\bar{B}_r^{(2)} \in \mathbb{R}^{4\times 4}$, $\bar{B}_r^{(3)}$, $\bar{B}_r^{(4)} \in \mathbb{R}^{2\times 4}$, $\bar{C}_r^{(1)}$, $\bar{C}_r^{(2)} \in \mathbb{R}^{1\times 4}$, $\bar{C}_r^{(3)}$, $\bar{C}_r^{(4)} \in \mathbb{R}^{1\times 2}$, $\bar{D}_r^{(1)}$, $\bar{D}_r^{(2)} \in \mathbb{R}^{4\times 1}$, $\bar{D}_r^{(3)}$, $\bar{D}_r^{(4)} \in \mathbb{R}^{2\times 1}$. The multiplicative uncertainties $\Delta_m^{(i)}(s)$ due to model reduction are described as

$$\Delta_m^{(i)}(s) = \frac{P_f^{(i)}(s) - P_r^{(i)}(s)}{P_r^{(i)}(s)}, \tag{20}$$

where $P_f^{(i)}(s)$ and $P_r^{(i)}(s)$ denote the transfer functions of the full order and the reduced order systems such as $P_f^{(i)}(s) = \bar{C}_f^{(i)}(sI - \bar{A}_f^{(i)})^{-1}\bar{B}_f^{(i)}$, $P_r^{(i)}(s) = \bar{C}_r^{(i)}(sI - \bar{A}_r^{(i)})^{-1}\ \bar{B}_r^{(i)}$. It may be thought that the total uncertainty stems not only from the truncated modes in model reduction but also from unmodelled high-frequency modes larger than 500 Hz. As stated before, the level of the unmodelled modes would always be lower than modelled ones. Therefore, it will be a correct approach to consider only the truncated modes for uncertainty modelling.

3.2. CONTROL OBJECTIVES

The control system considered here is a regulator-type system with no reference input to be followed during control operation. The regulator problem considered in H_∞ control theory is how to construct a controller that stabilizes the closed-loop system and minimizes the H_∞ norm of the closed-loop system transfer function [13]. The first objective of the H_∞ control design will be robust stabilization of the feedback control system against the unknown multiplicative perturbation. Consider the block diagram of the control system shown in Figure 3 (a) and 3(b). There are two fundamental transfer functions in this control system structure. These are

$$M(s) = \frac{P_r(s)}{I - P_r(s)K(s)}, \qquad T(s) = \frac{P_r(s)K(s)}{I - P_r(s)K(s)}, \tag{21}$$

where $M(s)$ is called the settling function and $T(s)$ is called the complementary sensitivity function. In general, $T(s)$ is the main transfer function for evaluating the robust stability of a closed-loop system. Assuming that $T(s)$ and $\Delta_m^{(i)}(s)$ are both stable, the sufficient condition for the feedback system to be robustly stable against all perturbations is

$$\| W_T(s)T(s) \|_\infty < 1 \tag{22}$$

provided that the upper limit of $\Delta_m^{(i)}(s)$ satisfies

$$\bar{\sigma}[\Delta_m^{(i)}(s)] < W_T(s), \tag{23}$$

where $\bar{\sigma}$ indicates maximum singular value and $W_T(s)$ represents a weighting function for the transfer function $T(s)$. From equation (22), it is obvious that the smaller $T(s)$ is, the better the robust stability.

The second objective of the H_∞ control design is to improve the performance of the feedback control system. The problem in improving the response performance is how to attenuate the influence of the disturbance v on the output y of the plant. This issue is related to minimization of $\| M(s) \|_\infty = \sup \bar{\sigma}[M(s)]$ subject to the condition of stability of the closed-loop system. In practice, the influence of disturbance is relatively large in the

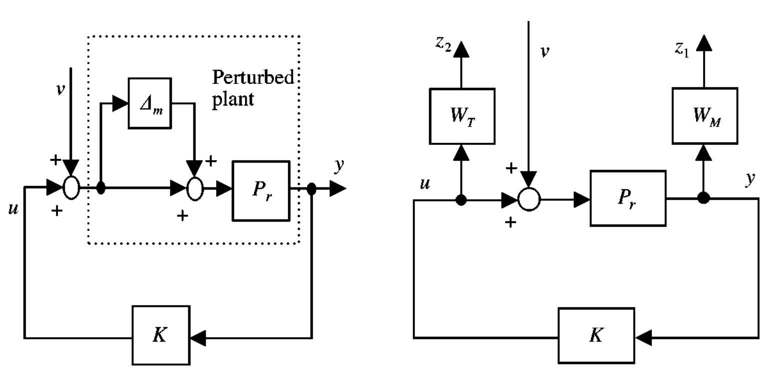

Figure 3. Block diagrams for H_∞ control design: (a) perturbed system, (b) augmented structure (z_1 and z_2 are controlled outputs).

low-frequency domain and relatively small in high frequency. Assuming that a weighting function $W_M(s)$ for the transfer function $M(s)$ is chosen to be large in the low-frequency domain, the H_∞ norm of the $\| W_M(s)M(s) \|_\infty$ will be small enough for disturbance attenuation.

Supposing that the weighting functions $W_T(s)$ and $W_M(s)$ are specified so that the control system satisfies both robust stabilization and response performance, the H_∞ control design for the mixed sensitivity problem is defined as

$$\left\| \begin{matrix} W_T(s)T(s) \\ W_M(s)M(s) \end{matrix} \right\|_\infty < 1. \tag{24}$$

3.3. SELECTION OF THE FREQUENCY SHAPING FILTERS

An important stage in H_∞ design is to select the frequency weighting functions. In this design study, the robust stabilization is mainly focused and improvement in response performance is satisfied by selecting a constant value for related weighting function such as $W_M = k_m$. A general rule to select the cross-over frequencies of W_T is to use the multiplicative uncertainty existing in the plant. In general, the uncertainties should be covered by the weighting function W_T to maintain robust stability. This rule needs to be revised by specifying some parameters that increase effectiveness of the design because there are infinite number of weighting filters which satisfy the condition of uncertainty covering. Here, an approach for selection of the frequency shaping filter W_T will be described for odd/odd mode group. The same approach is also valid for other mode groups. Since each state space has four input channels, the robust stability related weighting function has the structure of $W_T = \mathrm{diag}(w_T, w_T, w_T, w_T)$. A second order filter is defined as follows:

$$w_T = k_t \frac{s^2 + 2\xi_{wn}\omega_{wn}s + \omega_{wn}^2}{s^2 + 2\xi_{wd}\omega_{wd}s + \omega_{wd}^2}, \tag{25}$$

where subscripts *wn* and *wd* indicate the parameters of the filter for the numerator and the denominator respectively. The selection of the filter may be reduced to a single parameter such as k_t, provided that the frequency and damping values are specified. For odd/odd mode case, it is desired that controller gain should be high until the second odd/odd mode for suppressing the targeted two modes only. At the third and other odd/odd modes, the controller should be low gain for the sake of robustness. In the light of these design requirements, the corner frequencies of the filter become the second controlled mode and the third uncontrolled mode such as $\omega_{wn} = 89$ Hz, $\omega_{wd} = 199$ Hz. Damping rates are specified as $\xi_{wn} = 0{\cdot}5$, and $\xi_{wd} = 0{\cdot}2$. For different values of k_t $(0{\cdot}1 \leqslant k_t \leqslant 10)$, weighting filters are obtained and controllers are designed using these filters as shown in Figures 4(a) and 4(b) respectively. For small values of k_t such as 0·1, controller gain increases and excites higher order uncontrolled modes as shown in Figures 4(c) and 4(d) from the closed-loop system responses.

The design of the controllers were performed using the control architecture presented in Figure 3(b). Based on this structure, the augmented system for the control design may be obtained as

$$\begin{aligned} \begin{bmatrix} z_2 \\ z_1 \\ y \end{bmatrix} &= \begin{bmatrix} 0 & W_T(s) \\ W_M(s)P_r(s) & W_M(s)P_r(s) \\ P_r(s) & P_r(s) \end{bmatrix} \begin{bmatrix} v \\ u \end{bmatrix} \\ &= G(s) \begin{bmatrix} v \\ u \end{bmatrix}, \end{aligned} \tag{26}$$

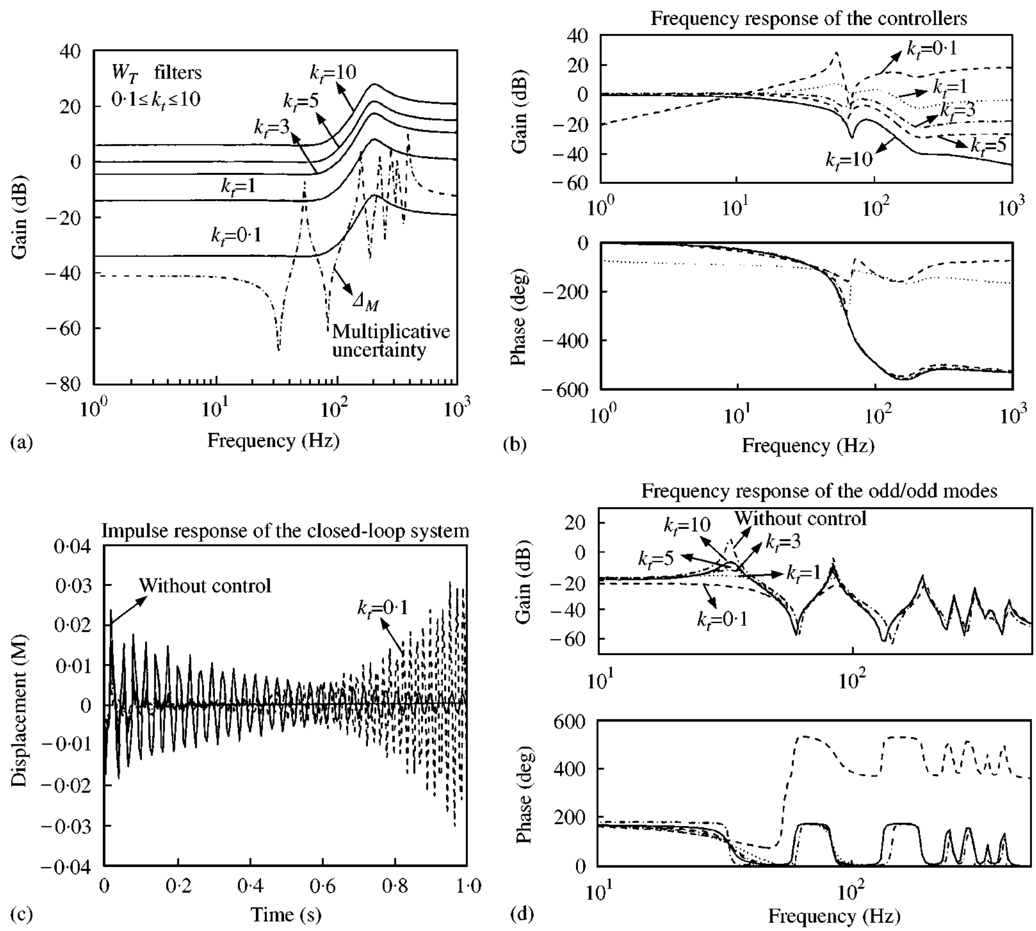

Figure 4. Frequency weighting filters and closed-loop responses: (a) weighting filters; (b) H_∞ controllers; (c) impulse responses; (d) closed-loop responses.

where $G(s)$ denotes the augmented plant matrix. For $W_M = k_m$ and $W_T = C_{wT}(sI - A_{wT})^{-1} B_{wT} + D_{wT}$, the augmented plant matrix $G(s)$ is obtained as

$$G(s) = \left[\begin{array}{cc|c|c} A_{wT} & 0 & 0 & B_{wT} \\ 0 & \bar{A}_r & \bar{B}_r & \bar{B}_r \\ \hline C_{wT} & 0 & 0 & D_{wT} \\ 0 & k_m\bar{C}_r & 0 & 0 \\ \hline 0 & \bar{C}_r & 0 & 0 \end{array}\right]$$

$$= \left[\begin{array}{c|cc} A & B_1 & B_2 \\ \hline C_1 & D_{11} & D_{11} \\ C_2 & D_{21} & D_{22} \end{array}\right]. \tag{27}$$

Forming the above augmented plant matrix for each mode group, the controllers were designed using the Matlab LMI Control Toolbox [12].

4. EXPERIMENTS

A previously constructed test system which is situated in a semi-anechoic room is used for control study and experiments. A flat steel plate measuring $1800 \times 880 \times 9\ \mathrm{mm}^3$ was supported on knife edges fixed to the perimeter of an enclosure with ferroconcrete walls of 10 cm thickness as illustrated in Figure 1. Inside the enclosure covered with absorbent material, an electro-dynamic shaker was installed to excite the plate. Distributed parameters sensors (totally 14 PVDF films) shaped for separating structural modes of the panel are attached to the structure. Four-point actuators fixed on U profile steel beams are placed over the panel structure at the corners. A feedback control system is established with a digital signal processor (DSP) to realize the experiments.

The steel panel is disturbed by white noise up to a frequency range of 500 Hz. Outputs from the shaped PVDF sensors attached to the plate are fed directly into the controllers as

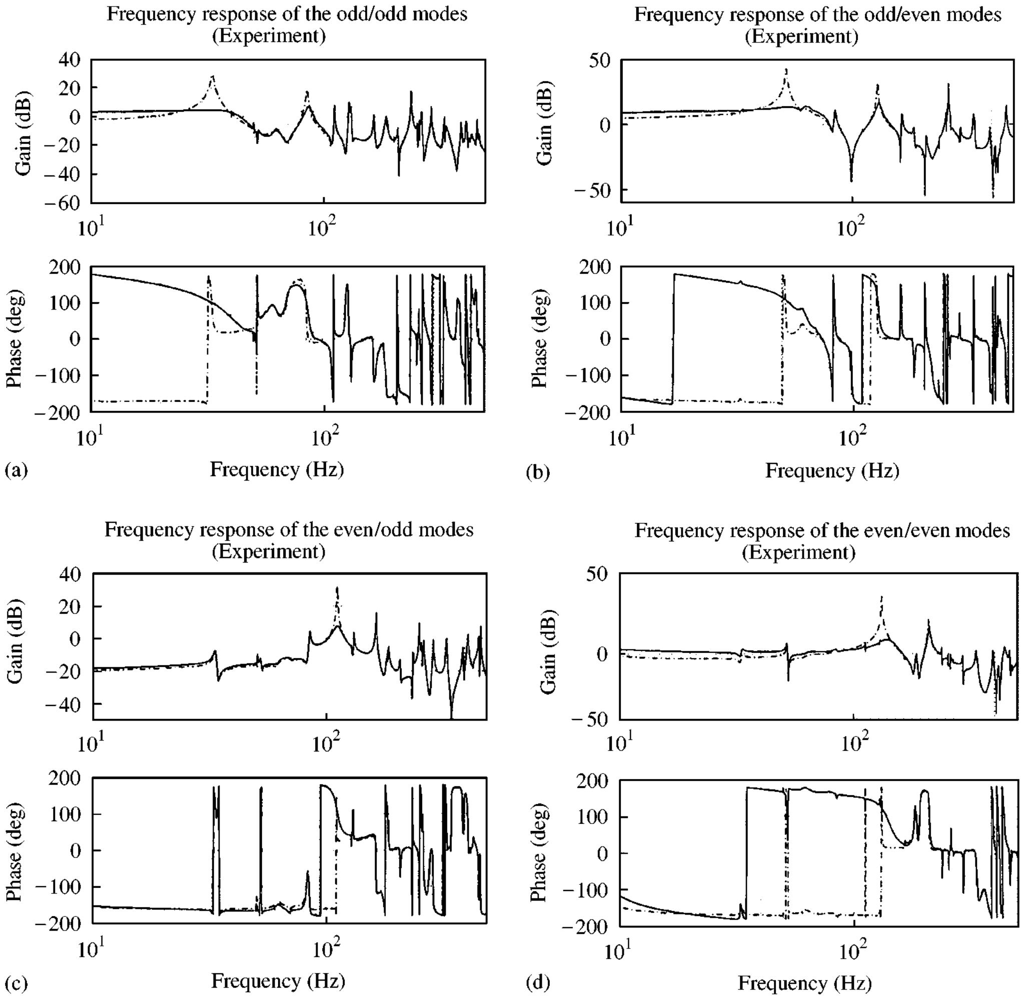

Figure 5. Frequency response of the closed-loop: (a) odd/odd modes: -·-·-·, without control; ——, with control; (b) odd/even modes: -·-·-·, without control; ——, with control; (c) even/odd modes: –·–·–, without control; ——, with control; (d) even/even modes: –·–·–, without control; ——, with control.

error signals. The computed H_∞ controllers for odd/odd, odd/even, even/odd and even/even modes are discretized and downloaded into four DSP running in parallel. Note that all controllers run simultaneously and the outputs of the controllers are summed at each channel before feeding through power amplifiers to the actuators. The actuators suppress panel vibration to minimize the noise radiated by the vibrating panel.

Figure 5(a–d) shows the experimental results achieved by the H_∞ feedback controllers for each mode groups. Compared with or without control case shown in Figure 5(a), the targeted (1, 1) and (1, 3) odd/odd modes with control are suppressed 21·76 and 9·16 dB respectively. The controlled (1, 2) and (1, 4) odd/even modes decreased 28·74 and 14·85 dB, respectively, as shown in Figure 5(b). Similarly, the targeted (2, 1) even/odd mode and (2, 2) even/even mode suppressed 24·49 and 32·09 dB (Figures 5(c–d)). In all these results, the uncontrolled modes larger than 150 Hz are not excited by H_∞ feedback controllers. The time history responses of the control system are presented in Figure 6(a–d). The time history responses with control show significant decrease in the displacement amplitude of the plate. The suppression of the acoustic power mode results in the spectrum shown in Figure 7, which is obtained by the acoustic power measurement using a microphone traversing system set 10 cm from the panel. The results obtained with acoustic power measurements in Figure 7 agreed with the results obtained in Figure 5(a–d) except some increase in power modes close to 163 and 259 Hz. A possible explanation of these increases is that they are caused by external effects such as power modes of the beams, which are used for supporting

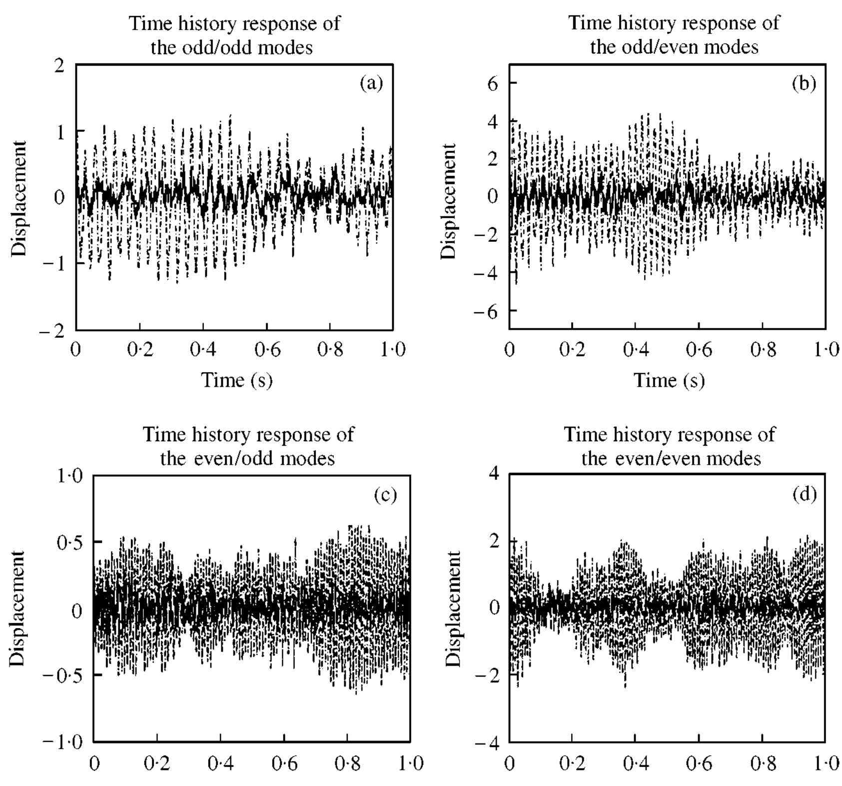

Figure 6. Time history responses: (a) Odd/odd modes: $-\cdot-\cdot-$, without control; ——, with control. (b) Odd/even modes: ----, without control; ——, with control. (c) Even/odd modes: -----, without control; ——, with control. (d) Even/even modes: $-\cdot-\cdot-$, without control; ——, with control.

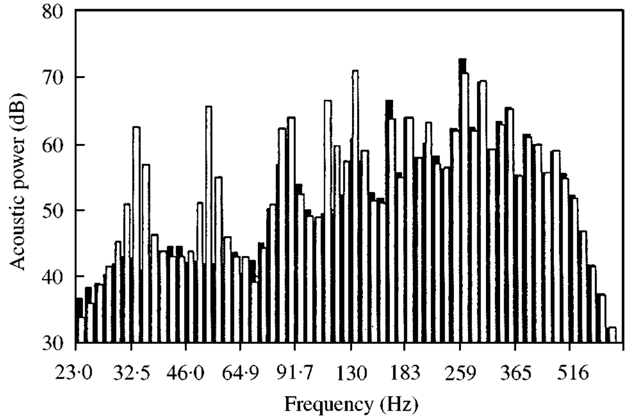

Figure 7. Acoustic power spectra: ■, with control; □, without control.

the actuators, because there is no increase in attached PVDF sensor outputs in this frequency range.

5. CONCLUSIONS

Output feedback control of acoustic power radiated from a planar structure using H_∞ control theory has been described. The state-space equations of a panel structure for odd/odd, odd/even, even/odd and even/even modal groups are derived and transformed in order to suppress radiated acoustic power. The output equations of the state spaces are formed using distributed parameter modal sensors. An H_∞ control design is explained based on the reduced order model by introducing the truncated high-frequency modes as multiplicative uncertainties. Experiments on active modal control are conducted using H_∞ robust controllers, showing a significant reduction of the targeted modal amplitudes without exciting the uncontrolled modes of the structure.

REFERENCES

1. C. R. FULLER, C. H. HANSEN and S. D. SNYDER 1991 *Journal of Sound and Vibration* **150**, 179–190. Experiments on the active control of sound radiation from a panel using piezo ceramic actuator.
2. R. L. CLARK and C. R. FULLER 1992 *Journal of the Acoustical Society of America* **91**, 3321–3329. Modal sensing of efficient acoustic radiators with PVDF distributed sensors in active structural approaches.
3. S. D. SNYDER, N. TANAKA and Y. KIKUSHIMA 1995 *American Society of Mechanical Engineers Journal of Vibration and Acoustic* **117**, 311–322. The use of optimally shaped piezoelectric film sensors in the active control of free field structural radiation. Part 1: feedforward control.
4. S. D. SNYDER, N. TANAKA and Y. KIKUSHIMA 1996 *American Society of Mechanical Engineers Journal of Vibration and Acoustics* **118**, 112–121. The use of optimally shaped piezo-electric film sensors in the active control of free field structural radiation. Part 2: feedback control.
5. C. GUIGOU, A. BERRY and F. CHARETTE 1994 *Proceedings of the American Society of Mechanical Engineers Winter Annual Meeting* AD-vol. 45/MD-vol54, 247–255. Active control of plate volume velocity using shaped PVDF sensor.
6. G. P. GIBBS, R. L. CLARK, D. E. COX and J. S. VIPPERMAN 2000 *Journal of the Acoustical Society of America* **107**, 332–339. Radiation modal expension: application to active structural acoustic control.

7. R. L. Clark, W. R. Saunders and G. P. Gibbs 1997 *Adaptive Structures: Dynamics and Control*. New York: Wiley.
8. N. Tanaka, S. D. Snyder and C. H. Hansen 1996 *American Society of Mechanical Engineers Journal of Vibration and Acoustics* **118**, 630–640. Distributed parameter modal filtering using smart sensor.
9. N. Tanaka, Y. Kikushima and N. J. Ferguson 1998 *Journal of the Acoustical Society of America* **104**, 217–225. One-dimensional distributed parameter sensors and the active modal control for planar structures.
10. S. Sivrioglu, Y. Kikushima and N. Tanaka 1999 *Proceedings of the* 6*th International Congress on Sound and Vibration*, 1669–1676. An H_∞ control design approach for distributed parameter structures with attached PVDF sensors.
11. J. C. Doyle, B. A. Francis and A. R. Tannenbaum 1992 *Feedback Control Theory*. New York: Macmillan Publishing Company.
12. P. Gahinet, A. Nemirovski, A. J. Laub and M. Chilali 1995 *Mathworks*. LMI control toolbox, for use with MATLAB.
13. M. Sampei, T. Mita and M. Nakamichi 1990 *Systems and Control Letters* **14**, 13–24. An algebric approach to H_∞ output feedback control problems.